Electrochimica Acta 56 (2010) 804–809

Contents lists available at ScienceDirect

Electrochimica Acta

journal homepage: www.elsevier.com/locate/electacta

Effect of zwitterionic salt on the electrochemical properties of a solid polymer electrolyte with high temperature stability for lithium ion batteries

Z.H. Li[a,*,1], Q.L. Xia[a], L.L. Liu[a], G.T. Lei[a], Q.Z. Xiao[a], D.S. Gao[a], X.D. Zhou[b]

[a] *Key Laboratory of Environmentally Friendly Chemistry and Applications of Ministry of Education, College of Chemistry, Xiangtan University, Hunan 411105 China*
[b] *State Key Laboratory of Chemical Engineering, East China University of Science and Technology, Shanghai 200237 China*

ARTICLE INFO

Article history:
Received 9 June 2010
Received in revised form
15 September 2010
Accepted 18 September 2010
Available online 25 September 2010

Keywords:
Ionic liquid
Polymer electrolyte
Lithium ion batteries
Ionic conductivity
Zwitterionic salt

ABSTRACT

In this study, we prepare a kind of solid polymer electrolyte (SPE) based on *N*-ethyl-*N*′-methyl imidazolium tetrafluoroborate ($EMIBF_4$), $LiBF_4$ and poly(vinylidene difluoride-co-hexafluoropropylene) [P(VdF-HFP)] copolymer. The resultant SPE displays high thermal stability above 300 °C and high room temperature ionic conductivity near to $10^{-3}\,S\,cm^{-1}$. Its electrochemical properties are improved with incorporation of a zwitterionic salt 1-(1-methyl-3-imidazolium)propane-3-sulfonate (MIm3S). When the SPE contains 1.0 wt% of the MIm3S, it has a high ionic conductivity of $1.57 \times 10^{-3}\,S\,cm^{-1}$ at room temperature, the maximum lithium ions transference number of 0.36 and the minimum apparent activation energy for ions transportation of $30.9\,kJ\,mol^{-1}$. The charge–discharge performance of a $Li_4Ti_5O_{12}$/SPE/$LiCoO_2$ cell indicates the potential application of the as-prepared SPE in lithium ion batteries.

1. Introduction

Lithium ion batteries (LIBs) have been widely used as power sources for many portable electronics such as laptop computer, digital camera and mobile phone owing to their high energy density and long life. In general, the conventional LIBs use the solution of lithium salt in alkyl carbonates as electrolyte, which will be evaporated into gas at elevated temperature. The aggregation of gas in battery case results in some serious accidents such as burn and explosion. Therefore, the LIBs suffer from a safety problem when they operate at elevated temperature that might come from their operation at larger current density or improper uses such as overcharge, over-discharge and short-circuit. The safety problem of the LIBs would be solved if the nonaqueous electrolyte were replaced with solid polymer electrolyte or room temperature ionic liquid (RTIL) [1]. RTIL, which is nonvolatile and nonflammable, has been used as a plasticizer to incorporate the SPE to enhance the ionic conductivity. Of the most important, the safety of LIBs can be guaranteed with use of RTIL [2–15].

$EMIBF_4$ with low viscosity has a high ionic conductivity of $14 \times 10^{-3}\,S\,cm^{-1}$ at 25 °C [16], which is similar to those of the classical electrolytes based on lithium salts in the mixtures of alkyl carbonates. Moreover, it shows an electrochemical window about 4.0 V and a high thermal decomposition temperature more than 300 °C. The incorporation of $EMIBF_4$ into polymer matrix can enhance the ionic conductivity of the resultant SPE [17–22], but the SPE incorporated with much $EMIBF_4$ is poor in mechanical strength [23]. In addition, lithium salt must be added to the polymer electrolyte because it is Li^+ ions not EMI^+ ions intercalate the electrode materials in LIBs. In this case, the migration cations in the lithium salt–RTIL–polymer ternary system (i.e. the RTIL-plasticized SPE) include both Li^+ and EMI^+ ions in a potential gradient [2]. The competition of EMI^+ ions with Li^+ ions does decrease the lithium ions transference number of the obtained polymer electrolyte [24]. Ogihara et al. reported that the addition of lithium salt led to a decrease of ionic conductivity of the RTIL-plasticized SPE [25]. Fortunately, it has been reported that the addition of the zwitterionic compounds based on pyrrolidinium or imidazolium assists in the dissociation of Li^+ ions [12,26] and the formation of the solid electrolyte interface (SEI) film in the RTIL–zwitterions-based electrolyte or polymer electrolyte [27–29]. However, few of papers discuss the effect of zwitterionic salt (MIm3S) on the electrochemical properties of the P(VdF-HFP)-based polymer electrolyte that is plasticized with $EMIBF_4$.

Here we synthesize a zwitterionic salt, MIm3S to incorporate the P(VdF-HFP)-based SPE plasticized with $EMIBF_4$, and investigate its effect on the electrochemical properties of the obtained SPE such as ionic conductivity, lithium ions transference number and apparent activation energy for ions transportation. In addition,

---

* Corresponding author. Tel.: +86 731 58292206; fax: +86 731 58292251.
E-mail address: lzh69@xtu.edu.cn (Z.H. Li).

[1] ISE member.

0013-4686/$ – see front matter © 2010 Elsevier Ltd. All rights reserved.
doi:10.1016/j.electacta.2010.09.068

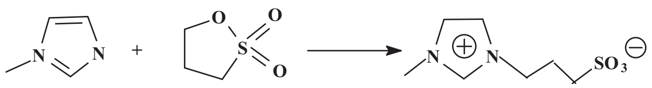

Scheme 1. Structure of the 1-(1-methyl-3-imidazolium)propane-3-sulfonate.

some $Li_4Ti_5O_{12}$/SPE/$LiCoO_2$ cells are fabricated to evaluate the possible application of the as-prepared SPE in LIBs.

2. Experimental

1-(1-Methyl-3-imidazolium)propane-3-sulfonate was synthesized according to a similar method described in the literature [30]. Typically, 4.0 g (42.0 mmol) 1-methyl imidazole (Alfa Aesar) was added dropwise to the solution of 5.0 g (42.0 mmol) 1,3-propanesultone (Alfa Aesar) in 100 ml acetone at first (the solution has been degassed with N_2 at 0 °C for 1 h at prior). The mixture was then stirred at room temperature for 100 h in a N_2 atmosphere. After that, the solution was filtered and the precipitate was purified twice with acetone and dried at 80 °C for 24 h in vacuum. Finally, 8.3 g white powders (MIm3S) were obtained (yielding ratio: 93%). The synthesis route is described in Scheme 1.

^{1}H NMR data of the as-prepared white powder: 2.5 (s, 3H), 7.67 (s, 1H), 7.76 (s, 1H), 9.09 (s, 1H), 2.43–2.40 (t, 2H), 2.13–2.06 (m, 2H), 4.33–4.29 (t, 2H).

FTIR data of the as-prepared white powder: 3154 cm^{-1} (C–H stretching), 3014 cm^{-1} (CH_2 stretching vibrations of the alkane) [31], 1646 cm^{-1} (stretching vibrations of the quaternary ammonium salt), 1575 cm^{-1}(C–C, C–N in-plane stretching vibrations of the cyclic imidazole) [32], 1392 cm^{-1} (CH_2 wagging), 1362 cm^{-1} (shoulder peaks, stretching vibrations of cyclic imidazole), 1337 cm^{-1} (CH_2 twisting) [33], 1194, 1043 cm^{-1} (S=O stretching vibrations of sulfate group) [34], 1172 cm^{-1} (C–H in-plane deformed vibration of cyclic imidazole) [32], 847 and 623 cm^{-1} (C–H out-plane bending vibrations of cyclic imidazole), 745 and 648 cm^{-1} (C–H out-plane bending vibrations of EMI^+) [35].

A mixed solution of 0.50 g $EMIBF_4$ (Alfa Aesar), 0.05 g $LiBF_4$ (Shanghai China Lithium Industry Co., Ltd.) and 0.50 g P(VdF-HFP) (Kynar Flex® 2801) in 4.50 ml *N*-methyl pyrrolidone (NMP) was produced at first. Various amounts (0, 0.016, 0.032 and 0.048 g, corresponding to 0, 1.0, 2.0 and 3.0 wt% of in the obtained SPE, respectively.) of the MIm3S was then dissolved in the above solution. The resultant viscous solution was spread on a glass plate and dried at 80 °C for 24 h in vacuum. Due to evaporation of the NMP, a self-supporting polymer membrane formed on the glass plate and was immediately transferred into a dry glove-box (H_2O content less than 5 ppm). The elastic polymer membrane was pouched into discs forming the SPE samples finally.

The melting point of the synthesized MIm3S was measured using the differential scanning calorimeter (DSCQ10, Perkin-Elmer) in the temperature range of 80–250 °C at a scan rate of 10 °C min^{-1} in a nitrogen atmosphere. The thermal decomposition temperatures of the as-prepared SPE and the MIm3S were determined through the thermogravimetric (TG) analysis at a heating rate of 10 °C min^{-1} in a nitrogen atmosphere.

In a dry glove-box, the SPE sample was sandwiched between two symmetrical lithium electrodes and encapsulated into a module cell. The electrochemical impedance spectra (EIS) were taken using an EG&G M273 Potentiostat/Galvanostat in conjunction with M5210 Lock-in amplifier electrochemical analysis system in the frequency range of 10^{-1}–10^5 Hz. The ionic conductivity of the SPE can be calculated from the equation $\sigma = d/(R_b \times S)$, where σ, R_b, d and S are the ionic conductivity, the bulk resistance, the thickness of the SPE membrane and the area of the lithium electrode, respectively.

The alter current (AC)/direct current (DC) method, which has been elucidated in detail by Bruce and Vincent [36], was widely used to determine the lithium ions transference number (t_+) of the RTIL–lithium salt–polymer system [37–42] thus the t_+ of the SPE in this study can be calculated from Eq. (1):

$$t_+ = \frac{I_s(\Delta V - I_0 R_{ct}^0)}{I_0(\Delta V - I_s R_{ct}^s)} \tag{1}$$

In Eq. (1), I_0 and I_s are the initial and the steady state currents measured by a DC polarization method, respectively. $R_{ct}{}^0$ and $R_{ct}{}^s$ are the charge transfer resistances at the initial and steady states, respectively. Their values can be determined from the Nyquist curves of the SPE before and after the DC polarization measurement. ΔV (50 mV) is an imposed potential difference between two lithium electrodes.

Linear sweep voltammetry (LSV) experiments were performed to investigate the electrochemical stability of the SPE using a three-electrode cell with stainless steel working electrode and lithium reference and counter electrodes. All experiments were carried out at a sweep rate of 10 mV s^{-1} in the potential range of 0–6 V (vs. Li/Li^+) at 25 °C.

Galvanostatic curves of the $Li_4Ti_5O_{12}$/SPE/$LiCoO_2$ cells were achieved using Arbin BT2000 battery tester. A slurry of $LiCoO_2$, acetylene black and poly(vinylidene difluoride) with a mass ratio of 85:10:5 in NMP was coated onto an aluminum sheet, and dried at 120 °C overnight under vacuum forming the cathode. The anode, which consists of 80 wt% of $Li_4Ti_5O_{12}$, 15 wt% of acetylene black and 5 wt% of PVDF, was prepared using copper sheet according to the process of cathode. The SPE containing 1 wt% of the MIm3S was sandwiched between the cathode and anode and encapsulated into a 2016-type coin cell. The cell was charged and discharged at a constant current in the output potential difference range of 1.1–2.6 V at 25 °C.

3. Results and discussion

Fig. 1 shows the differential scanning calorimetry (DSC) and thermogravimetric (TG) curves of the synthesized MIm3S (a) and the TG curves of the pure P(VdF-HFP) membrane and the as-prepared SPE (b). It can be seen that, from Fig. 1a, the melting temperature and the thermal decomposition temperature of the MIm3S are 222 and 357 °C, respectively. The thermal decomposition temperature of the pure P(VdF-HFP) is 478 °C and those of the solid polymer electrolytes (SPEs) incorporated without and with 1 wt% of the MIm3S are 353 and 341 °C, respectively. The thermal decomposition temperatures of the SPEs containing other amounts of the MIm3S are summarized in Table 1. It suggests that the thermal decomposition temperature of the SPE hardly varies with the amount of the zwitterionic salt, indicating that the lithium ion batteries using this kind of SPE would be safe even at high temperature (more than 300 °C).

The bulk resistance (R_b) and the charge transfer resistance (R_{ct}) of the SPEs can be obtained from the Nyquist curves (Fig. 2). The semicircle relating to the resistance component corresponds to the charge transfer and the capacity component to the electric double layer when non-blocking electrodes (i.e. lithium electrodes) are used [43]. In the low frequency range, the straight line declining about 45 degrees represents the Warburg impedance (Z_w) based on the diffusion of ions. The left intercept of the semicircle on the Z' axis represents the bulk resistance (R_b) of the SPE, while the right one equals to the sum of the R_b and R_{ct}. The equivalent circuit of the Li/SPE/Li cell is depicted in Fig. 2 (insertion). Table 1 presents the room temperature ionic conductivities of the SPEs containing various amounts of the MIm3S. It is found that the ionic conductivity of the SPE without the MIm3S is 0.59×10^{-3} S cm^{-1} and increases

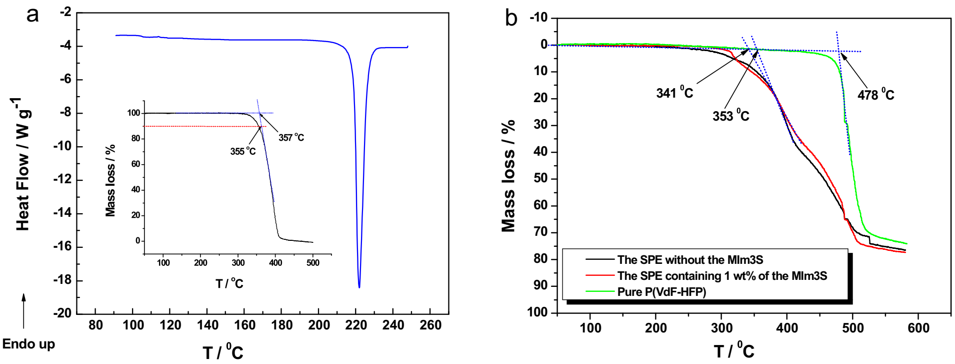

Fig. 1. (a) Differential scanning calorimetry and thermogravimetric curves of the 1-(1-methyl-3-imidazolium)propane-3-sulfonate measured in a N_2 atmosphere at a scan rate 10 °C min^{-1}. (Insert: thermogravimetric curve); (b) Thermogravimetric curves of the solid polymer electrolytes incorporated without and with 1.0 wt% of the 1-(1-methyl-3-imidazolium)propane-3-sulfonate.

Table 1
The thermal decomposition temperatures and the electrochemical properties of the solid polymer electrolytes incorporated with various amounts of the 1-(1-methyl-3-imidazolium)propane-3-sulfonate (MIm3S).

Content of the MIm3S (wt%)	Thermal decomposition temperature (°C)	Room temperature ionic conductivity (10^{-3} S cm^{-1})	Apparent activation energy for ions transportation (kJ mol^{-1})	Lithium ions transference number
0	353	0.59	39.0	0.19
0.5	347	0.78	38.7	0.24
1.0	341	1.57	30.9	0.36
2.0	338	1.01	37.7	0.25
3.0	330	0.41	43.3	0.10

firstly with the amount of MIm3S and then decreases with excessive incorporation. The ionic conductivity reaches the maximum value, 1.57×10^{-3} S cm^{-1} when the SPE contains 1.0 wt% of the MIm3S.

To elucidate the stability of the SPE with respect to metallic lithium, the dependence of the interfacial resistances (R_i) of the Li/SPE/Li cell on storage time is shown in Fig. 3. The interfacial resistance of the SPE without the MIm3S increases gradually within 24 h, and changes hardly in the time range of 24–104 h, then increases slightly with further storage. With incorporation of the MIm3S, the SPE reaches a stable value of the interfacial resistance after 8 h storage because the zwitterionic salt might react with the lithium electrode to form a solid electrolyte interface (SEI) film on its surface [29]. Thus, all the electrochemical measurements of the overall SPE samples were carried out after 24 h storage in this study.

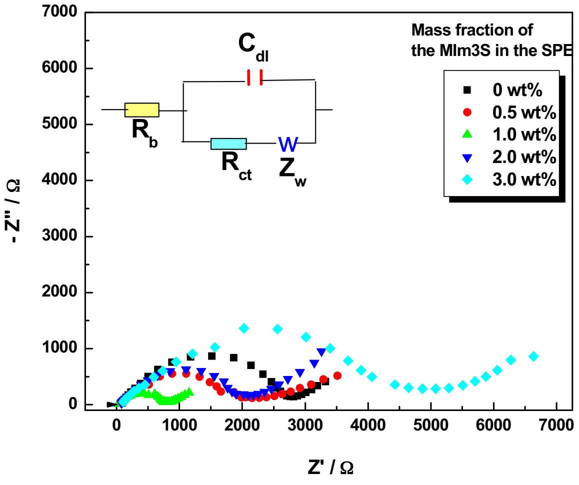

Fig. 2. Nyquist curves of the solid polymer electrolytes containing various amounts of the 1-(1-methyl-3-imidazolium)propane-3-sulfonate at room temperature. (Insert: equivalent circuit of the Li/SPE/Li cell).

Fig. 4 displays the chronoamperometry profile (a) and the Nyquist plots (b) of the SPE containing 1.0 wt% of the MIm3S. From Fig. 4a, we can find that I_0 and I_s of the SPE are 51 and 25 μA, respectively. Fig. 4b reveals that $R_{ct}{}^0$ and $R_{ct}{}^s$ are 750 and 1368 Ω, respectively. Thus, the lithium ions transference number (t_+) is calculated to be 0.36 according to Eq. (1). The other t_+ values of the SPEs are summarized in Table 1. It suggests that the lithium ions transference number increases at first and then decreases with the amount of the MIm3S. The lithium ions transference number reaches the maximum value when the SPE contains 1.0 wt% of the MIm3S.

In the as-prepared SPE, Li$^+$ ions are surrounded by a large number of $BF_4{}^-$ anions forming an ionic cluster, which absorbs many EMI$^+$ ions forming a large ionic atmosphere. Li$^+$ ions are trapped in the ionic atmospheres and migrate difficultly resulting in a low ionic conductivity and small lithium ions transference number. With incorporation of the zwitterionic salt (MIm3S), the compe-

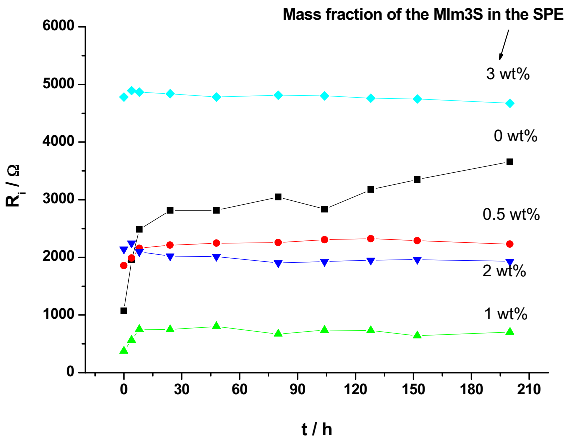

Fig. 3. Interfacial resistances of the solid polymer electrolytes incorporated with various amounts of the 1-(1-methyl-3-imidazolium)propane-3-sulfonate at room temperature after different storage time.

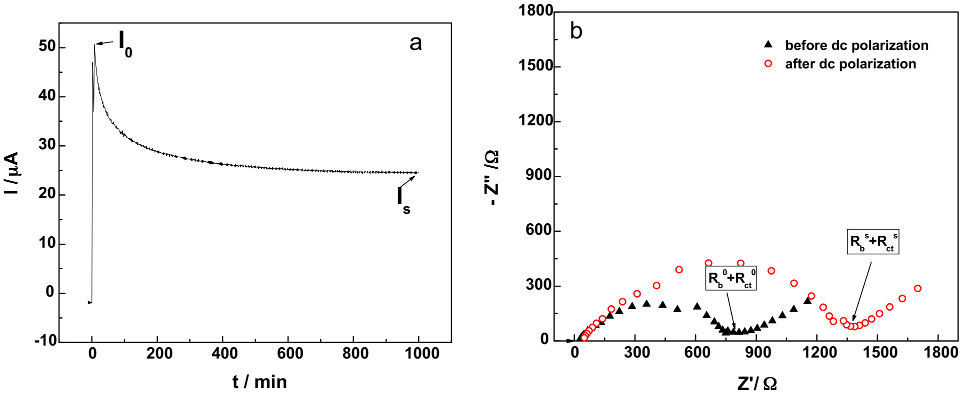

Fig. 4. Chronoamperometry profile (a) and Nyquist plots (b) of the solid polymer electrolytes containing 1.0 wt% of the 1-(1-methyl-3-imidazolium)propane-3-sulfonate at room temperature.

tition of the dissociated SO_3^- anions with Li^+ and EMI^+ ions maybe destroys the ionic atmospheres and thus Li^+ ions migrate easily. As a result, the ionic conductivity and the lithium ions transference number increase. Nevertheless, Li^+ ions will be surrounded by a large numbers of SO_3^- anions forming another ionic atmosphere if excessive MIm3S is incorporated into the SPE. Thus, the ionic conductivity and the lithium ions transference number decrease on the contrary. The incorporation of a suitable amount of the MIm3S into the SPE facilitates the dissociation of the lithium salt in fact.

Fig. 5 shows the dependence of the ionic conductivity of the SPE on temperature ($\log\sigma$–T^{-1} plots). We can see that the ionic conductivity increases with the increasing temperature and all the plots appear linear in the temperature range measured. In a wide temperature range, the conductive behavior of ions in polymer electrolyte usually obeys the VTF (Vogel–Tamman–Fulcher) relation $\sigma=\sigma_0\exp(-E_a/R(T-T_0))$, where T_0 is the idealized glass transition temperature of the polymer and is lower than that of the polymer by 20–50 K. Since the glass transition temperature of P(VdF-HFP) is −100 °C [44], T_0 will be far below the measure temperature range of 25–55 °C. Therefore, VTF behavior can be modeled as Arrhenius behavior whose equation is:

$$\sigma=\sigma_0\exp\left(\frac{-E_a}{RT}\right) \qquad (2)$$

where E_a, R and T are the apparent activation energy for ion transportation, the gas constant and the absolute test temperature, respectively. E_a calculated from Eq. (2) is 39.0 kJ mol^{-1} for the SPE without the MIm3S and decreases with the amount of the MIm3S (see Table 1) suggesting that the ions in the SPE containing the MIm3S migrate more easily than those in the SPE without the MIm3S. When the SPE contains 1.0 wt% of the MIm3S, E_a reaches the minimum value, 30.9 kJ mol^{-1}. On the contrary, it increases with excessive addition of the MIm3S (more than 1.0 wt%).

Fig. 6 shows the linear sweep votammogroms of the SPEs incorporated with various amounts of the MIm3S at a scan rate of 10 mV s^{-1} at room temperature. The SPE without the MIm3S exhibits a cathodic limit at 0.72 V (vs. Li/Li$^+$) and an anodic limit at 4.91 V (vs. Li/Li$^+$). When incorporated with 0.5, 1.0, 2.0, and 3.0 wt% of the MIm3S, the SPEs display the cathodic limits of 0.67, 0.49, 0.28 and 0.18 V (vs. Li/Li$^+$), respectively, and the corresponding anodic limits are 5.07, 5.36, 5.35 and 5.25 V (vs. Li/Li$^+$). It can be seen that the cathodic stability versus lithium of the SPE is improved with incorporation of the zwitterionic salt. The zwitterionic salt (MIm3S) facilitates the formation of the SEI film on the surface of Li electrode and thus the EMI^+ ions can hardly contact with Li electrode. Consequently, the electrochemical stability of this kind of SPE is improved although $EMIBF_4$ is used.

It has been reported that the cathodic limit of the pure $EMIBF_4$ is about 1.0 V (vs. Li/Li$^+$), which is caused by the presence of the acidic C-2 hydrogen atom in the imidazolium heterocycle [45–49]. Some improvements on the electrochemical stability of imidazolium have been achieved by substituting C-2 hydrogen with an alkyl

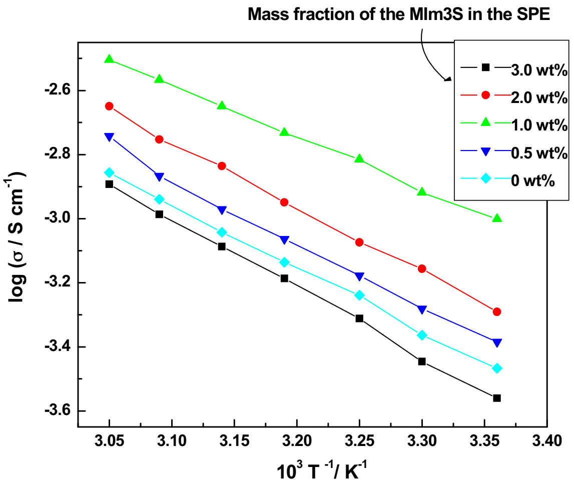

Fig. 5. $\log\sigma$–T^{-1} curves of the solid polymer electrolytes incorporated with various amounts of the 1-(1-methyl-3-imidazolium)propane-3-sulfonate in the range of 25–55 °C.

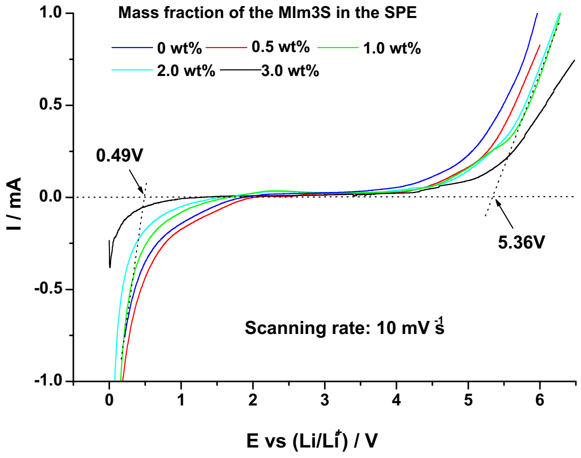

Fig. 6. Linear sweep voltammograms of the solid polymer electrolytes incorporated with various amounts of the 1-(1-methyl-3-imidazolium)propane-3-sulfonate at a sweep rate of 10 mV s^{-1} at room temperature. (Working electrode: stainless steel; reference and counter electrodes: lithium).

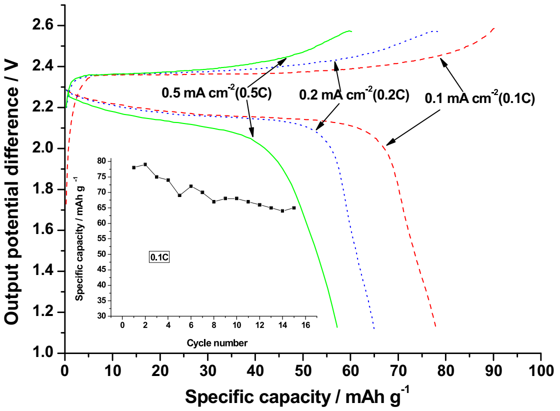

Fig. 7. Galvanostatic curves of the $Li_4Ti_5O_{12}$/SPE/$LiCoO_2$ cell at various current densities of 0.1, 0.2 and 0.5 mA cm^{-2} at room temperature. The used solid polymer electrolyte contains 1 wt% of the 1-(1-methyl-3-imidazolium)propane-3-sulfonate. (Insert: cycle performance of the test cell at 0.1 °C).

group [5,50–53], or by adding the film-forming additives such as vinylene carbonate (VC) [54], fluoroethylene carbonate (FEC) [55], and γ-butyl olactone [56] into the imidazolium-based electrolyte. In addition, the lithium ion batteries that use the anode materials with high intercalation potential (vs. Li/Li$^+$) such as $Li_4Ti_5O_{12}$ [14,54–57], Mo_6S_8 [58] and MoO_2 [59] present good cycling performance.

Some persons have reported that the addition of lithium salt would make the cathodic limit of EMI$^+$ ions shift more negatively [59–61] and the polymer electrolyte containing EMI$^+$ ions showed high electrochemical stability [58,62]. In this study, the formed SEI film on the surface of electrode prevents EMI$^+$ ions from contacting lithium electrode. As a result, EMI$^+$ ions might not be reduced on the surface of lithium electrode and thus the electrochemical stability of SPE is improved.

Fig. 7 shows the galvanostatic curves of the $Li_4Ti_5O_{12}$/SPE/$LiCoO_2$ cell at various current densities at room temperature and its cycling performance (inset). The SPE containing 1 wt% of the MIm3S was used as the separator of the $Li_4Ti_5O_{12}$/SPE/$LiCoO_2$ cell. It reveals that the test cell delivers the capacities of 78, 65, and 57 mAh g^{-1} (based on the mass of $Li_4Ti_5O_{12}$) at the current densities of 0.1, 0.2 and 0.5 mA cm^{-2}, respectively. These capacities are much lower than the theoretical capacity of 175 mAh g^{-1}. Since lithium ions migrate more difficultly in the SPE compared with liquid electrolyte, they are not able to intercalate and de-intercalate the electrode materials promptly resulting in the large polarization resistance. In addition, the high interfacial resistance will consume a part of capacity when the cell is charged or discharged. Consequently, the test cell delivers lower capacity. The cycling performance of the test cell at 0.1C shows that the test cell is able to deliver a capacity of about 65 mAh g^{-1} in the 15th cycle. The results suggest that the as-prepared SPE should be applied in LIBs after further modification. The work is under way.

4. Conclusions

A zwitterionic-type ionic liquid, 1-(1-methyl-3-imidazolium)propane-3-sulfonate (MIm3S) has been synthesized successfully via one step and was incorporated into the P(VdF-HFP)-based SPE containing $EMIBF_4$ and $LiBF_4$. The resultant SPE showed a thermal decomposition temperature more than 300 °C. Since the zwitterionic salt would facilitate the formation of the SEI film on the surface of Li electrode and enhance the disassociation of lithium salt in the SPE, the electrochemical properties of the SPE were improved by incorporation of the MIm3S. When the SPE contained 1.0 wt% of the MIm3S, it had a room temperature ionic conductivity of 1.57×10^{-3} S cm^{-1} and a lithium ions transference number up to 0.36. At this amount, the SPE possessed the minimum value of the apparent activation energy for ions transportation, 30.9 kJ mol^{-1} and displayed an electrochemical stability in the potential range of 0.49–5.36 V (vs. Li/Li$^+$). The results of charge–discharge measurements of the $Li_4Ti_5O_{12}$/SPE/$LiCoO_2$ cell suggest a potential application of this kind of SPE in LIBs.

Acknowledgements

Financial support from the Natural Science Fund from Hunan Province (09JJ5008), the Open Fund from State Key Laboratory of Chemical Engineering in East China University of Science and Technology (SKL-ChE-08C06), and the Doctoral Starting Fund from Xiangtan University (05QDZ18) is greatly appreciated. We also thank Ms. M.N. Liu for her help in the DSC and TG measurements.

References

[1] M. Armand, F. Endres, D.R. MacFarlane, H. Ohno, B. Scrosati, Nat. Mater. 8 (2009) 621.
[2] A. Lewandowski, A. Świderska-Mocek, J. Power Sources 194 (2009) 601.
[3] I. Stępniak, E. Andrzejewska, Electrochim. Acta 54 (2009) 5660.
[4] B. Scrosati, J. Garche, J. Power Sources 195 (2010) 2419.
[5] K.S. Liao, T.E. Sutto, E. Andreoli, P. Ajayan, K.A. McGrady, S.A. Curran, J. Power Sources 195 (2010) 867.
[6] A. Guerfi, M. Dontigny, P. Charest, M. Petitclerc, M. Lagacé, A. Vijh, K. Zaghib, J. Power Sources 195 (2010) 845.
[7] M. Egashira, H. Todo, N. Yoshimoto, M. Morita, J. Power Sources 178 (2008) 735.
[8] Z.L. Tang, L. Qi, G.T. Gao, Solid State Ionics 180 (2009) 226.
[9] C. Sirisopanaporn, A. Fernicola, B. Scrosati, J. Power Sources 186 (2009) 490.
[10] A.L. Pont, R. Marcilla, I.D. Meatza, H. Grande, D. Mecerreyes, J. Power Sources 188 (2009) 558.
[11] J. Kagimoto, N. Nakamura, T. Kato, H. Ohno, Chem. Commun. 17 (2009) 2405.
[12] C. Tiyapiboonchaiya, J.M. Pringle, J. Sun, N. Byrne, P.C. Howlett, D.R. MacFarlane, M. Forsyth, Nat. Mater. 3 (2004) 29.
[13] M.A.B.H. Susan, T. Kaneko, A. Noda, M. Watanabe, J. Am. Chem. Soc. 127 (2005) 4976.
[14] A. Guerfi, M. Dontigny, Y. Kobayashi, A. Vijh, K. Zaghib, J. Solid State Electrochem. 13 (2009) 1003.
[15] H. Ye, J. Huang, J.J. Xu, A. Khalfan, S.G. Greenbaum, J. Electrochem. Soc. 154 (2007) A1048.
[16] M.J. Earle, J.M.S.S. Esperanca, A. Gilea, J.N.L. Canongia, L.P.N. Rebelo, J.W. Magee, K.R. Seddon, J.A. Widegren, Nature 439 (2006) 831.
[17] Y.P. Wang, X.H. Gao, J.C. Chen, Z.W. Li, C.L. Li, S.C. Zhang, J. Appl. Polym. Sci. 113 (2009) 2492.
[18] H. Nakajima, H. Ohno, Polymer 46 (2005) 11499.
[19] J.K. Kim, J. Manuel, G.S. Chauhan, J.H. Ahn, H.S. Ryu, Electrochim. Acta 55 (2010) 1366.
[20] H. Nakagawa, S. Izuchi, K. Kuwana, T. Nukuda, Y. Aihara, J. Electrochem. Soc. 150 (2003) A695.
[21] Y. Tominaga, M. Morita, S. Asai, M. Sumita, e-J Soft Mater. 1 (2005) 14.
[22] Z.H. Li, J. Jiang, G.T. Lei, D.S. Gao, Polym. Adv. Technol. 17 (2006) 604.
[23] T.E. Sutto, J. Electrochem. Soc. 154 (2007) 101.
[24] S.-Y. Lee, H.H. Yong, Y.J. Lee, S.K. Kim, S. Ahn, J. Phys. Chem. B 109 (2005) 13663.
[25] W. Ogihara, S. Washiro, H. Nakajima, H. Ohno, Electrochim. Acta 51 (2006) 2614.
[26] A. Narita, W. Shibayama, K. Sakamoto, T. Mizumo, N. Matsumi, H. Ohno, Chem. Commun. 18 (2006) 1926.
[27] J. Sun, D.R. MacFarlane, N. Byrne, M. Forsyth, Electrochim. Acta 51 (2006) 4033.
[28] N. Byrne, P.C. Howlett, D.R. MacFarlane, M. Forsyth, Adv. Mater. 17 (2005) 2497.
[29] N. Byrne, P.C. Howlett, D.R. MacFarlane, M.E. Smith, A. Howes, A.F. Hollenkamp, T. Bastow, P. Hale, M. Forsyth, J. Power Sources 184 (2008) 288.
[30] M. Yoshizawa, M. Hirao, K. Ito-Akita, H. Ohno, J. Mater. Chem. 11 (2001) 1057.
[31] T. Wiktor, J.W. Marek, J. Phys. Chem. A 107 (2003) 7827.
[32] N. Nanbu, Y. Sasaki, F. Kitamura, Electrochem. Commun. 5 (2003) 383.
[33] W.N. Richard, P.W. Faguy, S.C. Weibel, J. Eelectroanal. Chem. 448 (1998) 237.
[34] D. Stoilova, H.D. Lutz, J. Mol. Struct. 606 (2002) 267.
[35] J.A. Collado, I. Tunon, E. Silla, J. Phys. Chem. A 104 (2000) 2120.
[36] P.G. Bruce, C.A. Vincent, J. Electroanal. Chem. 225 (1987) 1.
[37] S. Kim, S.J. Park, Electrochim. Acta 54 (2009) 3775.
[38] H. Cheng, C.B. Zhu, B. Huang, M. Lu, Y. Yang, Electrochim. Acta 52 (2007) 5789.
[39] T. Mizumo, T. Watanabe, N. Matsumi, H. Ohno, Polym. Adv. Technol. 19 (2008) 1445.
[40] S. Ferrari, E. Quartarone, P. Mustarelli, A. Magistris, M. Fagnoni, S. Protti, C. Gerbaldi, A. Spinella, J. Power Sources 195 (2010) 559.
[41] E. Abitelli, S. Ferrari, E. Quartarone, P. Mustarelli, A. Magistris, M. Fagnoni, A. Albini, C. Gerbaldi, Electrochim. Acta 55 (2010) 5478.
[42] D. Bansal, F. Cassel, F. Croce, M. Hendrickson, E. Plichta, M. Salomon, J. Phys. Chem. B 109 (2005) 4492.

[43] P. Raghavan, X.H. Zhao, J. Manuel, G.S. Chauhan, J.H. Ahn, H.S. Ryu, H.J. Ahn, K.W. Kim, C. Nah, Electrochim. Acta 55 (2010) 1347.
[44] A. Kumar, M. Deka, S. Banerjee, Solid State Ionics 181 (2010) 609.
[45] M. Egashira, S. Okada, J. Yamaki, D.A. Dri, F. Bonadies, B. Scrosati, J. Power Sources 138 (2004) 240.
[46] M. Egashira, M. Nakagawa, I. Watanabe, S. Okada, J. Yamaki, J. Power Sources 146 (2005) 685.
[47] S. Seki, Y. Ohno, Y. Kobayashi, H. Miyashiro, A. Usami, Y. Mita, H. Tokuda, M. Watanabe, K. Hayamizu, S. Tsuzuki, M. Hattori, N. Terada, J. Electrochem. Soc. 154 (2007) A173.
[48] J.S. Lee, N.D. Quan, J.M. Hwang, J.Y. Bae, H. Kim, B.W. Cho, H.S. Kim, H. Lee, Electrochem. Commun. 8 (2006) 460.
[49] D.Q. Nguyen, J. Hwang, J.S. Lee, H. Kim, H. Lee, M. Cheong, B. Lee, H.S. Kim, Electrochem. Commun. 9 (2007) 109.
[50] S.H. Yeon, K.S. Kim, S. Choi, J.H. Cha, H. Lee, J. Phys. Chem. B 109 (2005) 17928.
[51] M.J. Monteiro, F.F.C. Bazito, L.J.A. Siqueira, M.C.C. Ribeiro, R.M. Torresi, J. Phys. Chem. B 112 (2008) 2102.
[52] N. Koura, K. Iizuka, Y. Idemoto, K. Ui, Electrochemistry 67 (1999) 706.
[53] J. Fuller, R.T. Carlin, R.A. Osteryoung, J. Electrochem. Soc. 144 (1997) 3881.
[54] M. Holzapfel, C. Jost, A. Prodi-Schwab, F. Krumeich, A. Wursig, H. Buqa, P. Novak, Carbon 43 (2005) 1488.
[55] I.A. Profatilova, N.S. Choi, S.W. Roh, S.S. Kim, J. Power Sources 192 (2009) 636.
[56] A. Chagnes, M. Diaw, B. Carré, P. Willmann, D. Lemordant, J. Power Sources 145 (2005) 82.
[57] B. Garcia, S. Lavallée, G. Perron, C. Michot, M. Armand, Electrochim. Acta 49 (2004) 4583.
[58] E. Markevich, V. Baranchugov, D. Aurbach, Electrochem. Commun. 8 (2006) 1331.
[59] J. Čaja, T.D.J. Dunstan, H.A. Dyar, H. Krall, V. Katović, Kem. Ind. 54 (2005) 205.
[60] M. Yamagata, Y. Fukuda, R. Tanaka, M. Ishikawa, ECS Trans. 16 (2008) 133.
[61] M. Morita, I. Murayama, T. Fukutake, N. Yoshimoto, M. Egashira, M. Ishikawa, ECS 210th Meeting, Abstract 0136.pdf.
[62] G. Cheruvally, J.K. Kim, J.W. Choi, J.H. Ahn, Y.J. Shin, J. Manuel, P. Raghavan, K.W. Kim, H.J. Ahn, D.S. Choi, C.E. Song, J. Power Sources 172 (2007) 863.